Supplementary Materials: Thermal effects on the lifetime of evaporating drops on fibers

M. Corpart[1,2], F. Restagno[1], and F. Boulogne[1]

[1]Université Paris-Saclay, CNRS, Laboratoire de Physique des Solides, 91405, Orsay, France.
[2]Corresponding author: marie.corpart@gmail.com

October 31, 2024

Appendix A: Materials and methods

1 Experimental setup

The experimental setup described in the main article, the homemade wind tunnel, is shown in more detail in Figure A.1. Figure A.1(a) shows a side view of the outside of the homemade wind tunnel and Figure A.1(b) provides a schematic view of the setup as well as a zoomed view of the drop placed on a fiber.

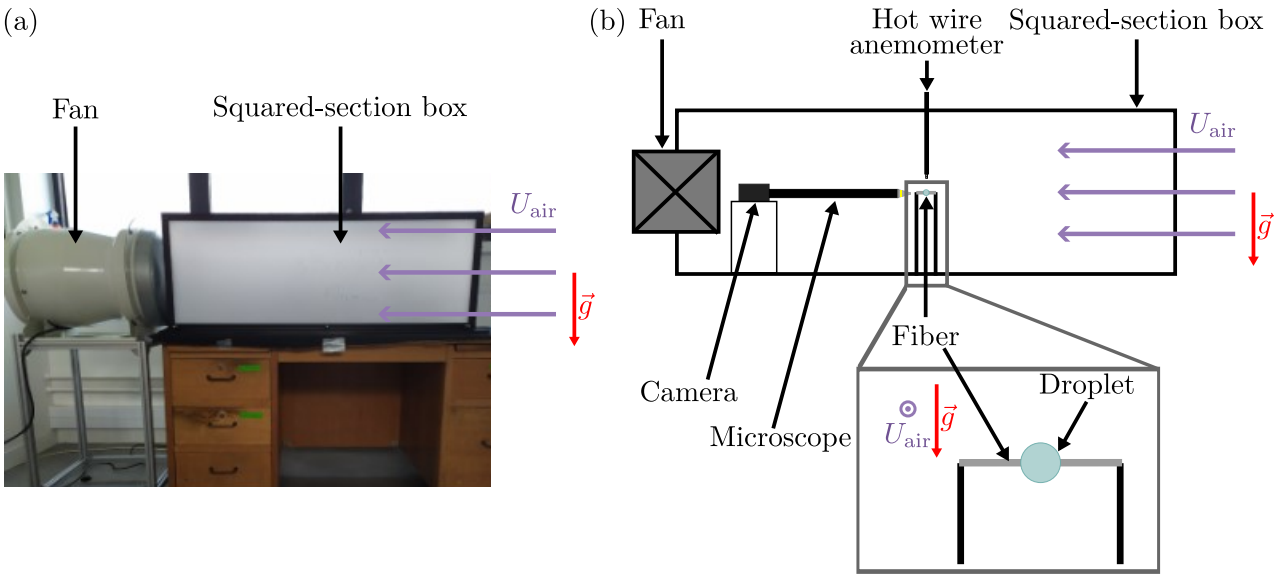

Figure A.1: (a) Photograph and (b) schematic representation of the homemade wind tunnel.

2 Morphologies of the drops on the fibers

All the lifetime measurements were obtained for drops adopting initially an axisymetric configuration, known as the barrell shape [1, 2, 3], on the fiber. The timelapses of a water drop on a glass (Fig. A.2(a)) and a copper fiber (Fig. A.2(b)) and a cyclohexane drop on a glass (Fig. A.2(c)) and a copper fiber (Fig. A.2(d)) evaporating in diffusive regime ($U_{air} = 0$) are shown in Figure A.2. Figure A.2 shows that all the liquids adopt a barrel configuratin on the tested fiber and the different wetting conditions have a small impact on the geometry of the liquid as expected for drop place on a fiber [1, 2, 3].

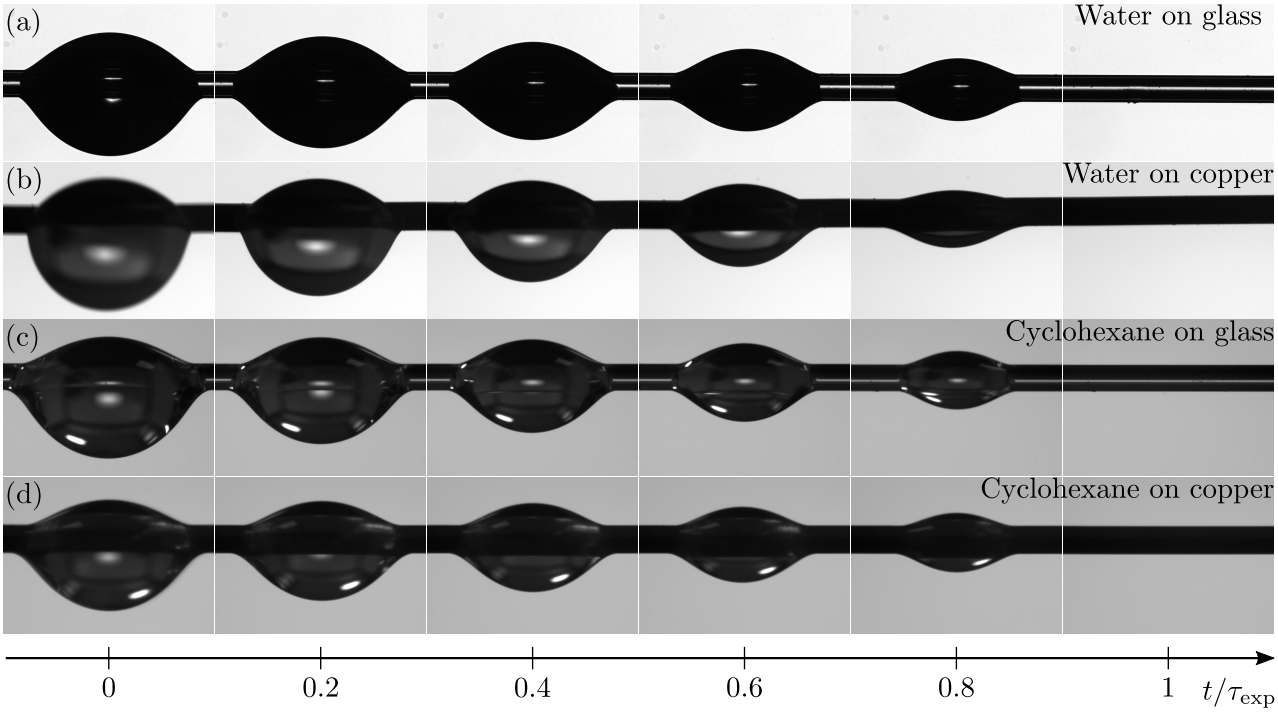

Figure A.2: Time-lapse of the evaporation of a drop of initial volume $\Omega_0 \approx 0.8$ µL deposited on a fiber of radius $a = 125$ µm observed in side view. (a) Water on glass fiber (same photos as in Figure 1(a) of the main text.), (b) water on copper fiber, (c) cyclohexane on glass fiber and (d) cyclohexane on copper fiber

All lifetime measurements were obtained for drops that initially adopt an axisymmetric configuration on the fiber, known as the barrel shape [1, 2, 3]. The time lapses of a water drop on glass (Fig. A.2(a)) and copper fiber (Fig. A.2(b)) and a cyclohexane drop on glass (Fig. A.2(c)) and copper fiber (Fig. A.2(d)) evaporating in the diffusive regime ($U_{\mathrm{air}} = 0$) are shown in Figure A.2. Figure A.2 shows that all liquids adopt a barrel configuration, kept throughout the evaporation, on the tested fiber and that the different wetting conditions have little effect on the geometry of the liquid, as expected for drops placed on a fiber [1, 2, 3].

Appendix B: Physicochemical properties of the studied liquids

In our experiments, temperature and relative humidity are variable. In Figure B.1, the lifetimes measured in the diffusive regime are plotted as a function of the relative humidity $\mathcal{R}_{\mathrm{H}}^{\mathrm{exp}}$. For water droplets, relative humidity is measured using a commercial hygrometer. Since there is no cyclohexane or octane vapor in the atmosphere, $\mathcal{R}_{\mathrm{H}}^{\mathrm{exp}} = 0$ for the alkanes. The color of the markers provides information about the air temperature away from the drop, T_{exp}, during the measurement of the lifetime of each individual drop.

The air temperature varies between 15 °C and 25 °C, which has a significant effect on the evaporation rate of the liquid and precludes direct comparison of results obtained for a given liquid/solid system at a constant relative humidity. This can be observed, for example, in B.1, where the data points representing the results obtained for a drop of water on a copper fiber (circles) at relative humidity $\mathcal{R}_{\mathrm{H}} \approx 35$ % are not superimposed because the temperature varies between 19 and 22 °C.

We thus need to calculate the theoretical lifetimes, predicted by our model, in the experimental conditions. To do so we need to prescribe the variation of several physical constant with the temperature as described in details in [4]. Here we summarize the phenomenological equations used to calculate the relevant parameters as well as some data extracted from the literature. We will consider the example of an isolated spherical droplet whose lifetime is determined by the combination of equations (2) and (6) of the main article. To calculate the lifetime for a given T_∞, we need the values of ρ, $\chi(T_\infty) =$

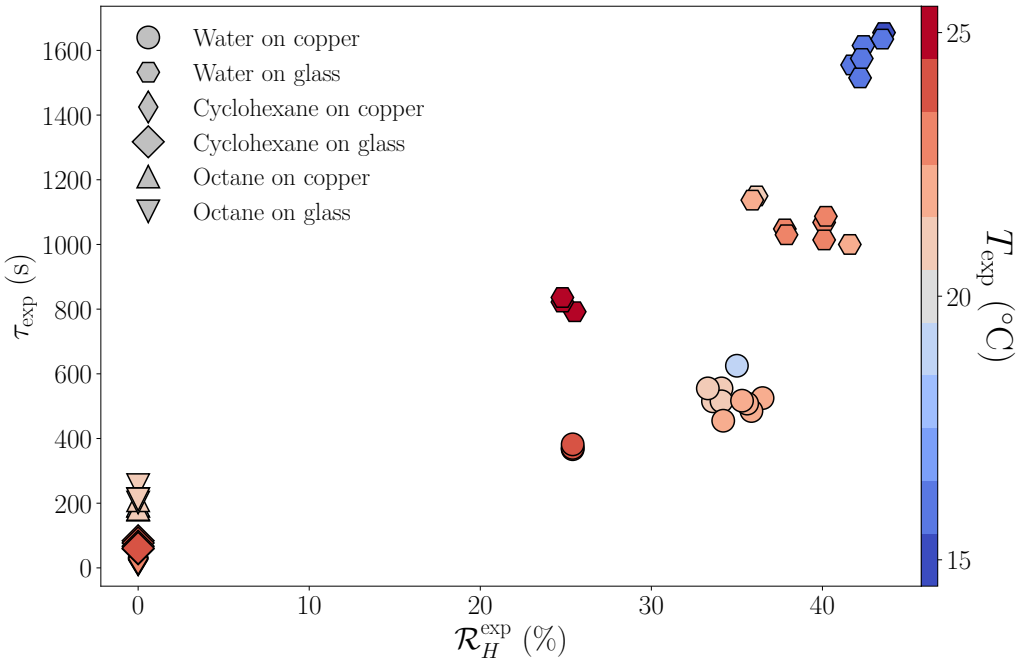

Figure B.1: Evolution of the measured lifetimes in diffusive regime ($U_{\mathrm{air}} = 0$) as a function of the ambient humidity and temperature conditions.

$\Delta_{\mathrm{vap}}H\mathcal{D}(T_\infty)c_{\mathrm{sat}}(T_\infty)/\lambda_{\mathrm{air}}(T_\infty)$, $\alpha_1(T_\infty)$ and $\alpha_2(T_\infty)$. We limit this study to ambient temperatures range, $T_\infty \in [0, 30]$ °C. In the following we review the temperature variations of all the submentioned parameters.

1 Density and enthalpy of vaporization

In the selected temperature range, the values of ρ and $\Delta_{\mathrm{vap}}H$ remain almost constant. Therefore, we have chosen to use their values at 20 and 25 °C, respectively, as these are the values commonly found in handbooks of physics. These data are gathered in the Table 1 for all the liquids studied.

	Water	Cyclohexane	Octane	Ref.
M (kg/mol)	18×10^{-3}	84×10^{-3}	114×10^{-3}	[5]
$\Delta_{\mathrm{vap}}H$ (J/kg)	2.44×10^{6}	3.93×10^{5}	3.64×10^{5}	[5]
ρ (kg/m^3)	998.2	779	702.5	[5]
V (cm^3/mol)	13.1	104.8	168.7	[6]

Table 1: Physical constants of the liquids under consideration, M is the molar mass and V the molecular volume as described in [6]. The mass density ρ is given for the liquid at 20 °C, while the enthalpy of vaporization $\Delta_{\mathrm{vap}}H$ is specified at 25 °C.

2 Diffusion coefficient $\mathcal{D}$

The value of the diffusion coefficient of vapor in air at T_∞ is estimated by the Fuller, Schettler, and Giddings' method [7, 6] which writes for a molecule A diffusing in B

$$\mathcal{D}(A,B) = \frac{T^{1.75}\sqrt{\frac{1}{M_{\mathrm{A}}} + \frac{1}{M_{\mathrm{B}}}}}{P_{\mathrm{atm}}\left(V_A^{1/3} + V_B^{1/3}\right)^2} \cdot 10^{-6}. \tag{1}$$

The diffusion coefficient $\mathcal{D}$ is expressed in m^2/s, the molar mass of compound i is in g/mol and V_i is the diffusion volume of the molecule i where $V_i = \sum_j n_j V_j$ with j a given atom composing the molecule [6]. The diffusion volume and molar masses of the molecules are given in Table 1 for the considered liquids.

3 *Saturating vapor concentration c_{sat} at T_∞*

To obtain the value of $c_{\text{sat}}(T_\infty)$, vapor is treated as an ideal gas, so the saturated vapor concentration $c_{\text{sat}}(T)$ is given by:

$$c_{\text{sat}}(T) = \frac{p_{\text{sat}}(T)M}{\mathcal{R}T}, \tag{2}$$

where p_{sat} represents the saturated vapor pressure, M is the molar mass of the vapor, $\mathcal{R}$ is the ideal gas constant, and T is the temperature in Kelvin. The temperature dependence of p_{sat} is approximated by Antoine's equation.

$$p_{\text{sat}}(T) = P^\circ \, 10^{A - \frac{B}{C+T}}, \tag{3}$$

where $P^\circ = 10^3$ Pa and T is in Kelvin.

The constants, A, B, and C, are determined by fitting the data extracted from literature for the considered liquids which are presented in Table B.3, with the Antoine's equation (Eq. (3)). Table 2 gathers the coefficients obtained for water, cyclohexane, and octane within the temperature range of $T \in [0, 30]$ °C.

	A	B	C
Water	7.34	1808	-33.9
Cyclohexane	6.17	1304	-40.4
Octane	11.2	4791	139

Table 2: Antoine's coefficients. The coefficients A, B, and C have been obtained by fitting the data extracted from the literature with the Antoine equation (Eq. (3)). Coefficients B and C are in Kelvin. The data are available in Table B.3. The coefficients given here are valid for temperatures in the range of $T \in [0, 30]$°C.

4 *Values of α_1 and α_2*

To perform analytically the calculation of droplet evaporation we choose to use an approximation to describe $c_{\text{sat}}(T)$. To model the temperature-dependent behavior of the saturation concentration, we employ a quadratic approximation (Eq. (5) of the main text), a method previously used in Ref. [4]. The coefficients α_1 and α_2 are determined for a given air temperature T_∞, by fitting the c_{sat} values obtained from the literature (Table B.3 combined with Eq. (2)). The resulting values are compiled in Table 4 for temperatures between 10 and 30 °C.

5 *Temperature variation of air thermal conductivity λ_{air}*

To calculate the value of λ_{air} at T_∞ we use Andreas [22] phenomenological equation for dry air,

$$\lambda_{\text{air}} = -3.47 \cdot 10^{-8} \, T^2 + 9.88 \cdot 10^{-5} \, T - 2.75 \cdot 10^{-4}, \tag{4}$$

which described with a good accuracy, the evolution of the air thermal conductivity with temperature as shown in [4]. The temperature is in Kelvin and the air thermal conductivity in $\text{W} \cdot \text{m}^{-1} \cdot \text{K}^{-1}$.

Water			Cyclohexane						Octane					
T (°C)	p_{sat} (Pa)	Ref	T (°C)	p_{sat} (Pa)	Ref	T (°C)	p_{sat} (Pa)	Ref	T (°C)	p_{sat} (Pa)	Ref	T (°C)	p_{sat} (Pa)	Ref
0	6.11×10^2	[5]	5.25	4.93×10^3	[8]	20.21	1.04×10^4	[8]	0	3.60×10^2	[9]	25.7	2.00×10^3	[10]
1	6.57×10^2	[5]	5.26	4.95×10^3	[8]	20.36	1.05×10^4	[8]	0	3.87×10^2	[9]	26.35	2.00×10^3	[10]
2	7.06×10^2	[5]	6.56	5.33×10^3	[8]	21.53	1.11×10^4	[8]	0	4.33×10^2	[11]	26.75	2.04×10^3	[12]
3	7.58×10^2	[5]	7.27	5.49×10^3	[8]	21.64	1.11×10^4	[8]	0	5.33×10^2	[11]	27.4	2.13×10^3	[13]
4	8.14×10^2	[5]	7.46	5.54×10^3	[8]	22.608	1.17×10^4	[14]	0	3.93×10^2	[11]	29.6	2.41×10^3	[13]
5	8.73×10^2	[5]	7.62	5.47×10^3	[8]	23.363	1.21×10^4	[14]	1.2	4.20×10^2	[12]	29.65	2.41×10^3	[12]
6	9.35×10^2	[5]	8.188	5.78×10^3	[14]	24.5	1.27×10^4	[8]	3.7	4.87×10^2	[11]	30	2.47×10^3	[15]
7	1.00×10^3	[5]	8.23	5.78×10^3	[8]	24.99	1.30×10^4	[8]	4.4	5.27×10^2	[12]			
8	1.07×10^3	[5]	8.59	5.88×10^3	[8]	25	1.30×10^4	[5]	5.26	5.32×10^2	[16]			
9	1.15×10^3	[5]	9.08	6.06×10^3	[8]	25	1.30×10^4	[17]	8.2	6.53×10^2	[12]			
10	1.23×10^3	[5]	9.698	6.24×10^3	[14]	25	1.30×10^4	[18]	9.25	7.13×10^2	[12]			
11	1.31×10^3	[5]	11.06	6.68×10^3	[8]	25	1.30×10^4	[19]	9.55	7.33×10^2	[12]			
12	1.40×10^3	[5]	11.13	6.70×10^3	[8]	25	1.30×10^4	[20]	11.2	8.20×10^2	[12]			
13	1.50×10^3	[5]	11.25	6.74×10^3	[8]	26.48	1.39×10^4	[8]	12.55	8.87×10^2	[12]			
14	1.60×10^3	[5]	11.356	6.79×10^3	[14]	27.42	1.45×10^4	[8]	14.35	9.93×10^2	[12]			
15	1.71×10^3	[5]	11.52	6.84×10^3	[8]	28.08	1.49×10^4	[8]	14.4	1.00×10^3	[5]			
16	1.82×10^3	[5]	12.17	7.07×10^3	[8]	28.346	1.51×10^4	[14]	16.41	1.05×10^3	[16]			
17	1.94×10^3	[5]	12.88	7.32×10^3	[8]	28.49	1.52×10^4	[8]	17.05	1.15×10^3	[12]			
18	2.06×10^3	[5]	14	7.73×10^3	[8]	28.97	1.55×10^4	[8]	18.1	1.25×10^3	[13]			
19	2.20×10^3	[5]	14.39	7.88×10^3	[8]	30	1.62×10^4	[21]	19.7	1.37×10^3	[12]			
20	2.34×10^3	[5]	14.59	7.98×10^3	[8]				20.05	1.47×10^3	[10]			
21	2.49×10^3	[5]	14.97	8.12×10^3	[8]				20.4	1.47×10^3	[10]			
22	2.64×10^3	[5]	15.07	8.15×10^3	[8]				20.7	1.45×10^3	[13]			
23	2.81×10^3	[5]	15.215	8.23×10^3	[14]				20.9	1.47×10^3	[10]			
24	2.99×10^3	[5]	17.163	9.04×10^3	[14]				23.15	1.65×10^3	[12]			
25	3.17×10^3	[5]	17.21	9.04×10^3	[8]				23.96	1.57×10^3	[16]			
26	3.36×10^3	[5]	18.18	9.48×10^3	[8]				24.6	1.82×10^3	[13]			
27	3.57×10^3	[5]	18.75	9.74×10^3	[8]				25	1.86×10^3	[5]			
28	3.78×10^3	[5]	19.3	1.00×10^4	[5]				25	1.86×10^3	[17]			
29	4.01×10^3	[5]	19.878	1.03×10^4	[14]				25	1.85×10^3	[9]			
30	4.25×10^3	[5]	20.11	1.04×10^4	[8]				25	1.87×10^3	[15]			

Table 3: Saturated vapor pressures p_{sat} as a function of temperature T for water, cyclohexane, and octane.

	Water		Cyclohexane		Octane	
T_∞ (°C)	α_1	α_2	α_1	α_2	α_1	α_2
10	-6.24×10^{-2}	1.41×10^{-3}	-4.91×10^{-2}	1.20×10^{-3}	-7.40×10^{-2}	3.14×10^{-3}
11	-6.17×10^{-2}	1.36×10^{-3}	-4.78×10^{-2}	9.64×10^{-4}	-7.04×10^{-2}	2.60×10^{-3}
12	-6.11×10^{-2}	1.32×10^{-3}	-4.70×10^{-2}	8.55×10^{-4}	-6.72×10^{-2}	2.19×10^{-3}
13	-6.04×10^{-2}	1.27×10^{-3}	-4.62×10^{-2}	7.88×10^{-4}	-6.45×10^{-2}	1.89×10^{-3}
14	-5.97×10^{-2}	1.23×10^{-3}	-4.56×10^{-2}	7.48×10^{-4}	-6.24×10^{-2}	1.66×10^{-3}
15	-5.91×10^{-2}	1.19×10^{-3}	-4.51×10^{-2}	7.20×10^{-4}	-6.05×10^{-2}	1.49×10^{-3}
16	-5.84×10^{-2}	1.15×10^{-3}	-4.46×10^{-2}	6.95×10^{-4}	-5.89×10^{-2}	1.35×10^{-3}
17	-5.77×10^{-2}	1.11×10^{-3}	-4.42×10^{-2}	6.76×10^{-4}	-5.79×10^{-2}	1.26×10^{-3}
18	-5.71×10^{-2}	1.07×10^{-3}	-4.37×10^{-2}	6.57×10^{-4}	-5.73×10^{-2}	1.20×10^{-3}
19	-5.64×10^{-2}	1.04×10^{-3}	-4.33×10^{-2}	6.40×10^{-4}	-5.64×10^{-2}	1.14×10^{-3}
20	-5.58×10^{-2}	1.01×10^{-3}	-4.28×10^{-2}	6.23×10^{-4}	-5.56×10^{-2}	1.08×10^{-3}
21	-5.52×10^{-2}	9.75×10^{-4}	-4.24×10^{-2}	6.06×10^{-4}	-5.44×10^{-2}	1.01×10^{-3}
22	-5.45×10^{-2}	9.45×10^{-4}	-4.20×10^{-2}	5.92×10^{-4}	-5.34×10^{-2}	9.56×10^{-4}
23	-5.39×10^{-2}	9.16×10^{-4}	-4.16×10^{-2}	5.79×10^{-4}	-5.26×10^{-2}	9.10×10^{-4}
24	-5.33×10^{-2}	8.88×10^{-4}	-4.12×10^{-2}	5.66×10^{-4}	-5.19×10^{-2}	8.74×10^{-4}
25	-5.27×10^{-2}	8.62×10^{-4}	-4.09×10^{-2}	5.52×10^{-4}	-5.15×10^{-2}	8.52×10^{-4}
26	-5.21×10^{-2}	8.36×10^{-4}	-4.05×10^{-2}	5.39×10^{-4}	-5.10×10^{-2}	8.28×10^{-4}
27	-5.15×10^{-2}	8.12×10^{-4}	-4.01×10^{-2}	5.27×10^{-4}	-5.05×10^{-2}	8.04×10^{-4}
28	-5.09×10^{-2}	7.88×10^{-4}	-3.98×10^{-2}	5.16×10^{-4}	-5.01×10^{-2}	7.82×10^{-4}
29	-5.04×10^{-2}	7.66×10^{-4}	-3.94×10^{-2}	5.05×10^{-4}	-4.96×10^{-2}	7.62×10^{-4}
30	-4.98×10^{-2}	7.44×10^{-4}	-3.91×10^{-2}	4.94×10^{-4}	-4.92×10^{-2}	7.42×10^{-4}

Table 4: Values of α_1 and α_2 for various temperatures T_∞ for water, cyclohexane, and octane.

Appendix C: Evaporation of a spherical drop

In this appendix we detail the calculations of evaporation of a spherical drop first in purely diffusive regime then under forced convection.

1 Diffusion-limited evaporation

Model We consider the mass transfer of the water vapor in the atmosphere surrounding a spherical drop of radius $R(t)$ and we assume that this process is limited by diffusion, which is valid in a quiescent atmosphere. This is true for droplet radius significantly larger than the mean-free path of the vapor molecules, *i.e.* R larger than few micrometers [23]. Over a timescale $R_0^2/\mathcal{D}$, where R_0 is the initial radius, the transfer can be considered to occur in a stationary regime. In practice, we can check that this timescale is short compared to the total evaporating time, such that the contribution of the starting non-stationary regime is negligible.

Thus, the concentration field c is the solution of the Laplace equation $\triangle c = 0$, which writes in spherical coordinates

$$\frac{1}{r^2}\frac{\mathrm{d}}{\mathrm{d}r}\left(r^2\frac{\mathrm{d}c}{\mathrm{d}r}\right) = 0. \tag{5}$$

This equation is supplemented by two boundary conditions on the concentration, respectively at the liquid-vapor interface and far from the interface,

$$c(r = R) = c_{\mathrm{sat}}(T_{\mathrm{i}}), \tag{6}$$
$$c(r \to \infty) = c_\infty, \tag{7}$$

where T_{i} is the temperature of the interface. The relative humidity is defined as $\mathcal{R}_{\mathrm{H}} = p_\infty/P_{\mathrm{sat}}(T_\infty) \approx c_\infty/c_{\mathrm{sat}}(T_\infty)$ in the ideal gas approximation, where T_∞ is the air temperature far from the droplet.

By integrating equation (5), the local evaporative flux given by Fick's law, $j = -\mathcal{D}\,\frac{\mathrm{d}c}{\mathrm{d}r}\big|_{r=R}$, writes

$$j = \mathcal{D}\frac{c_{\mathrm{sat}}(T_{\mathrm{i}}) - c_\infty}{R}. \tag{8}$$

The integration of the local flux over the evaporating surface gives $\Phi_{\mathrm{ev}} = \int j\,\mathrm{d}S = 4\pi R\mathcal{D}(T_{\mathrm{i}})(c_{\mathrm{sat}}(T_{\mathrm{i}}) - c_\infty)$, which can be rewritten

$$\Phi_{\mathrm{ev}} = 4\pi R\mathcal{D}c_{\mathrm{sat}}(T_\infty)\left(\frac{c_{\mathrm{sat}}(T_{\mathrm{i}})}{c_{\mathrm{sat}}(T_\infty)} - \mathcal{R}_{\mathrm{H}}\right). \tag{9}$$

where $\mathcal{D}$ is in good approximation the vapor diffusion coefficient at $T = T_\infty$ [4].

To compute the evaporation rate Φ_{ev} the temperature of the liquid must be determined. To do so, we write in the next paragraph the heat transfer between the atmosphere and the drop.

As for the mass transfer, we consider a diffusion limited process in a stationary regime, for which, the air temperature field is a solution of the Laplace equation $\triangle T = 0$ with the boundary conditions $T(r = R) = T_{\mathrm{i}}$ and $T(r \to \infty) = T_\infty$. The steady-state assumption also implies that the temperature in the drop has reached its equilibrium value T_{i} and is uniform in the liquid. This is validated if the timescale over which the heat diffuses through the liquid R_0^2/κ_ℓ with κ_ℓ the thermal conductivity of the liquid, is short compared to the evaporative time [24]. In practice, this is valid for the tested liquids evaporating under ambient conditions [25, 22, 24, 26, 27].

The integration of the Laplace equation leads to a total heat flux

$$Q_{\mathrm{h}} = -4\pi R\lambda_{\mathrm{air}}\Delta T^\star, \tag{10}$$

where $\Delta T^\star = T_\infty - T_{\mathrm{i}}$.

The heat and mass fluxes are coupled through the enthalpy of vaporization $\Delta_{\mathrm{vap}}H$, $\Delta_{\mathrm{vap}}H\,\Phi_{\mathrm{ev}} = -Q_{\mathrm{h}}$, which gives

$$\Delta T^\star = \chi\left(\frac{c_{\mathrm{sat}}(T_{\mathrm{i}})}{c_{\mathrm{sat}}(T_\infty)} - \mathcal{R}_{\mathrm{H}}\right), \tag{11}$$

with $\chi = \frac{\Delta_{\rm vap} H \mathcal{D} c_{\rm sat}(T_\infty)}{\lambda_{\rm air}}$ where $\Delta_{\rm vap} H$ is independent of the temperature (see Table 1), and the values of $\mathcal{D}, c_{\rm sat}(T_\infty)$ and $\lambda_{\rm air}$ are evaluated at $T = T_\infty$ by using the semi-empirical equations (1), (3) and (4) respectively.

To solve equation (11) we introduce a quadratic approximation of $c_{\rm sat}(T)$, defined as

$$c_{\rm sat}(T) = c_{\rm sat}(T_\infty)\left(1 + \alpha_1(T_\infty - T) + \alpha_2(T_\infty - T)^2\right), \tag{12}$$

where α_1 and α_2 are obtained by fitting the data from the literature (see Table 4). As discussed in [4], equation (12) is an excellent approximation of Antoine's equation (3).

Combining equations (11) and (12), we get

$$\chi\alpha_2 \Delta T^{\star 2} + (\chi\alpha_1 - 1)\,\Delta T^\star + \chi\,(1 - \mathcal{R}_{\rm H}) = 0. \tag{13}$$

Among the two roots admitted by equation (13), we keep the one for which $T_\infty - T_{\rm i}$ decreases as $\mathcal{R}_{\rm H}$ increases, *i.e.*

$$\Delta T^\star = \frac{1 - \chi\alpha_1 - \sqrt{(1-\chi\alpha_1)^2 - 4\chi^2\alpha_2\,(1-\mathcal{R}_{\rm H})}}{2\chi\alpha_2}. \tag{14}$$

Inserting the above expression into equation (9) we obtain the evaporation rate of the drop:

$$\Phi_{\rm ev} = 4\pi R \mathcal{D} c_{\rm sat}(T_\infty)\left[\alpha_2 \Delta T^{\star 2} + \alpha_1 \Delta T^\star + 1 - \mathcal{R}_{\rm H}\right], \tag{15}$$

with $\Delta T^\star$ given by equation (14).

The droplet lifetime is obtained from the conservation of the drop volume $\Omega = \frac{4}{3}\pi R^3$,

$$\Phi_{\rm ev} = -\rho \frac{{\rm d}\Omega}{{\rm d}t}, \tag{16}$$

where ρ is the liquid density. After integration from $R(0) = R_0$ to $R(\tau_{\rm S}) = 0$, we have the dynamics of the droplet radius $R(t) = R_0\sqrt{1 - t/\tau_{\rm S}}$, where the droplet lifetime is

$$\tau_{\rm S} = \frac{\rho R_0^2}{2\mathcal{D} c_{\rm sat}(T_\infty)\left(\alpha_2 \Delta T^{\star 2} + \alpha_1 \Delta T^\star + 1 - \mathcal{R}_{\rm H}\right)}, \tag{17}$$

with $\Delta T^\star$ given by equation (14). In the following we compare lifetimes of a spherical drop and a drop on a fiber in purely diffusive regime.

Comparison with experiments Figure C.1 shows a comparison between the measured lifetime of an axisymmetric drop on a fiber and the lifetime of a spherical drop evaporating under the same experimental conditions.

Figure C.1(a) shows the experimental lifetimes plotted against the lifetime of a spherical drop evaporating adiabatically ($T_{\rm i} = T_\infty$) under the same experimental conditions (liquid, initial volume, temperature, relative humidity). The dashed black curve in figure C.1(a) represents equality between the axes. As explained in the main text, the adiabatic model describes very well the experimental results obtained for all the liquids tested placed on a copper wire, as well as the results obtained for octane placed on a glass fiber. On the other hand, there is a systematic discrepancy between the ideal case of a spherical drop evaporating adiabatically and what is measured for a drop of water or cyclohexane placed on a glass fiber.

Figure C.1(b) displays the lifetime of different liquids evaporating on a glass fiber as a function of the lifetime of an airborne sphere composed of the same liquid, and cooling while evaporating under the same experimental conditions. The dotted curve represents axis equality. As mentioned in the main text, the presence of the fiber, even if it is made of an excellent thermal insulator, cannot be ignored in heat exchanges which explains that there is a systematic discrepancy between the experimental results obtained and the sphere model.

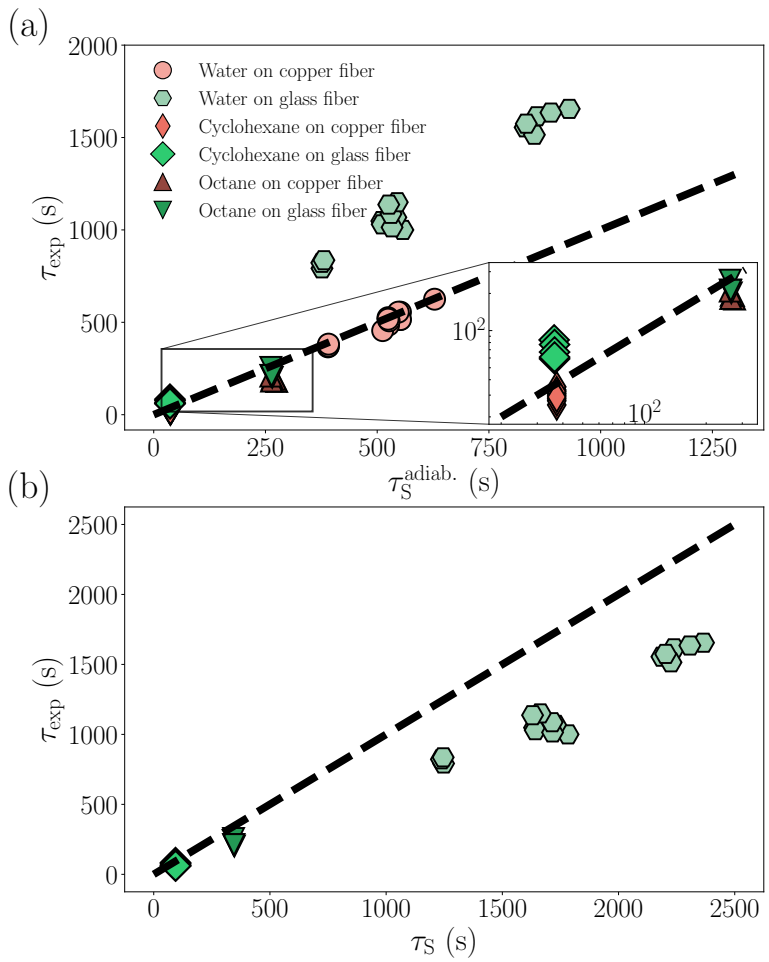

Figure C.1: Comparison between lifetime of an axisymmetric drop on a fiber and a spherical airborne drop evaporating in diffusive regime. (a) Measured lifetime of a drop on a fiber as a function of the lifetime of a spherical droplet (Eq. (17)) evaporating adiabatically ($T_i = T_\infty$) in the same conditions. (b) Measured lifetime of a drop on a glass fiber as a function of the lifetime of a spherical droplet (Eq. (17)) evaporating and exchanging heat with air in the same conditions. The temperature of the liquid is given by equation (14).

2 Forced-convective evaporation

We now turn to evaporation of a spherical drop under forced convection. As mentioned in the main text, Frössling [28] showed that the evaporation rate of a spherical drop placed in a laminar flow can be written as :

$$\Phi_{ev}^{conv} = \Phi_{ev} f_{ev}, \tag{18}$$

where Φ_{ev} is the purely diffusive evaporation rate (Eq. (9)) and f_{ev} the Sherwood number or the ventilation coefficient:

$$f_{ev} = 1 + \beta_{ev} \mathrm{Re}^{1/2} \mathrm{Sc}^{1/3} \tag{19}$$

Analogously, the convective heat flux received by the drop from the atmosphere can be written as follows [29, 30]:

$$Q_h^{conv} = Q_h f_h \tag{20}$$

with f_h the Nusselt number or ventilation coefficient

$$f_h = 1 + \beta_h \mathrm{Re}^{1/2} \mathrm{Pr}^{1/3}, \tag{21}$$

In the previous equations, $\mathrm{Re} = 2RU_{\mathrm{air}}/\nu_{\mathrm{air}}$ is the Reynolds number characteristic of the flow, $\mathrm{Sc} = \nu_{\mathrm{air}}/\mathcal{D}$ is the Schmidt number, $\mathrm{Pr} = \nu_{\mathrm{air}}/\alpha_{\mathrm{air}}$ is the Prandtl number and $\beta_{\mathrm{ev}} \approx \beta_{\mathrm{h}} \approx 0.3$ is a constant. In gases, $\mathrm{Pr} \approx \mathrm{Sc} \approx 1$ so $f_{\mathrm{ev}} \approx f_{\mathrm{h}}$.

Writing the energy balance $\Delta_{\mathrm{vap}} H \Phi_{\mathrm{ev}}^{\mathrm{conv}} = -Q_{\mathrm{h}}^{\mathrm{conv}}$ we obtain the liquid temperature:

$$\Delta T^\star = \chi \frac{f_{\mathrm{ev}}}{f_{\mathrm{h}}} \left(\frac{c_{\mathrm{sat}}(T_{\mathrm{i}})}{c_{\mathrm{sat}}(T_\infty)} - \mathcal{R}_{\mathrm{H}} \right), \tag{22}$$

which is virtually independent of air velocity and radius of the drop and approximately equal to the drop of temperature obtained in the purely diffusive regime (Eq. (11)) whose solution is given by equation (14). Integrating the mass conservation, $\Phi_{\mathrm{ev}}^{\mathrm{conv}} = -\rho \mathrm{d}\Omega/\mathrm{d}t$ we obtain the lifetime of the drop evaporating in forced convection:

$$\tau_{\mathrm{S}}^{\mathrm{conv}} = \frac{\rho}{\mathcal{D} c_{\mathrm{sat}}(T_\infty) \left(\alpha_2 \Delta T^{\star 2} + \alpha_1 \Delta T^\star + 1 - \mathcal{R}_{\mathrm{H}} \right)} \int_0^{R_0} \frac{r \mathrm{d}r}{1 + B r^{1/2}}, \tag{23}$$

where $B = \beta_{\mathrm{ev}} \mathrm{Sc}^{1/3} \sqrt{2U_{\mathrm{air}}/\nu_{\mathrm{air}}}$ and $\Delta T^\star$ is given by equation (14). The integration of the previous equation leads to the expression of the lifetime of the spherical drop of equation (17) of the main text.

Appendix D: Temperature of axisymmetric drop on a fiber

To predict the temperature of an axisymmetric drop on a fiber we study the model system of a spherical drop pierced by a fiber show in figure D.1. We adopt the hypotheses listed in the main text of the articles, and here we detail the resolution of equation (9) of the main text:

$$-2\pi a \, \lambda_{\mathrm{air}} \left. \frac{\mathrm{d}T}{\mathrm{d}r} \right|_{r=a} = \pi a^2 \lambda_{\mathrm{s}} \frac{\mathrm{d}^2 T}{\mathrm{d}z^2}. \tag{24}$$

The coordinate system is represented schematically in figure D.1(b). To solve this differential equation we must estimate the temperature gradient in air (left-hand side of equation (24)).

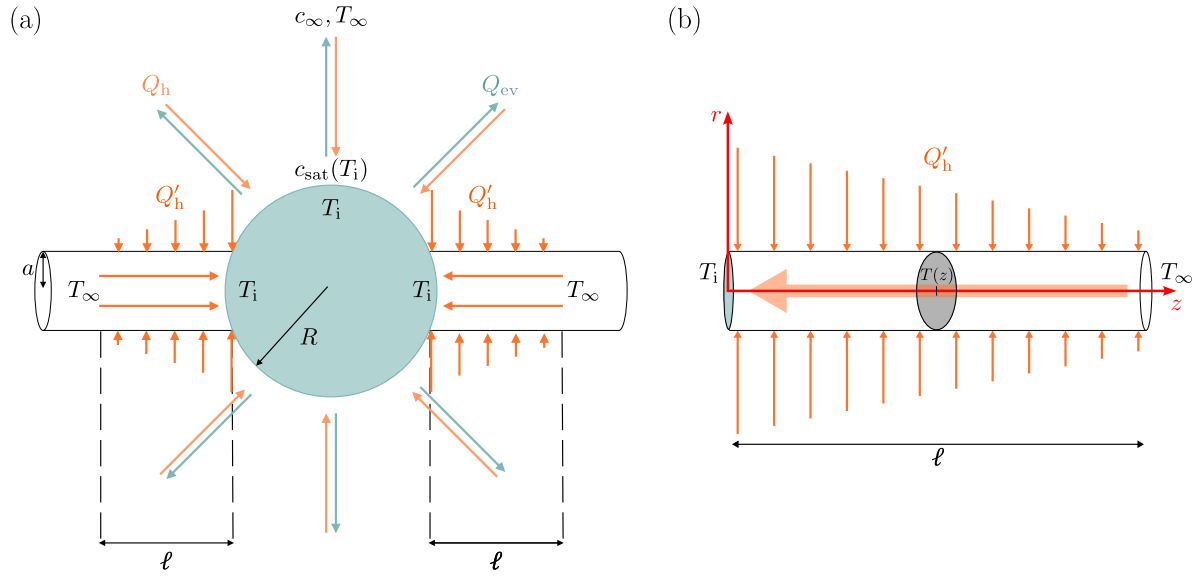

Figure D.1: (a) Schematic representation of the heat fluxes exchanged between the drop on a fiber and its environment. (b) Coordinate system used to calculate the temperature in the fiber.

In a previous work [31] we obtained analytically the surfacique evaporative flux of a liquid cylinder which is a problem analogous to the one that is considered here. We consider a cylinder of length $\ell \gg a$, shown in figure D.1(b), which receives a purely diffusive heat flux from the atmosphere with the following boundary conditions (i) the temperature at the surface of the dry fiber is equal to $T(z)$ and (ii) the temperature of the air far from the fiber is equal to T_∞. By analogy between mass and

heat transport, we can obtain the temperature gradient in air, evaluated at the surface of the fiber, in $r = a$, from equation (4) of [31]:

$$\left.\frac{\mathrm{d}T}{\mathrm{d}r}\right|_{r=a} = -\frac{\pi(T_\infty - T(z))}{2a\, f(\tilde{\ell}/2)}, \tag{25}$$

where $\tilde{\ell} = \ell/a$ and $f(x) = 2 - 2\gamma_e + \ln 2 + \frac{\pi}{2}\ln(x) \approx 10$, for $\ell \gg a$. As shown in [31], the previous equation describes very well the results obtained numerically for the evaporation of a sleeve of finite length and large aspect ratio (slender cylinder). Equation (25) is therefore expected to be a good approximation of the temperature gradient in air in the situation considered here. Inserting equation (25) into equation (24) and defining $\Theta(z) = T_\infty - T(z)$, we obtain the following differential equation:

$$\frac{\mathrm{d}^2\Theta}{\mathrm{d}z^2} = \frac{\Theta}{\mathcal{L}^2}, \tag{26}$$

whose solution is written

$$T_\infty - T(z) = (T_\infty - T_\mathrm{i}) \exp\left(-\frac{z}{\mathcal{L}}\right). \tag{27}$$

where the length $\mathcal{L}$ is given by:

$$\mathcal{L} \approx a\sqrt{\frac{10\lambda_\mathrm{s}}{\pi\lambda_\mathrm{air}}}. \tag{28}$$

Inserting equation (27) into $Q'_h = -\pi a^2 \lambda_\mathrm{s} \left.\vec{\nabla} T\right|_{z=0}$, (Eq (8) of the main text), we get the heat flux exchanged between the fiber and the drop on one side:

$$Q'_\mathrm{h} \approx -\pi a \Delta T^\star \sqrt{\frac{\pi\lambda_\mathrm{air}\lambda_\mathrm{s}}{10}}. \tag{29}$$

This calculation gives similar results to what was done by Fuchs [23] for a spherical drop suspended at the tip of a fiber. To solve equation (24), he considers an infinite cylinder and solves the Laplace's equation for the temperature in air by introducing a cut-off length which must be large compare to all the other lengths of the problem. The obtained heat flux exchanged between the fiber and the drop is similar to the result of equation (29) for a cut-off length equals to 500 times the radius of the fiber.

Inserting equation 29 into the globale energie balance of the system, $\Delta_\mathrm{vap}H$, $\Delta_\mathrm{vap}H\,\Phi_\mathrm{ev} = -(Q_\mathrm{h} + 2Q'_\mathrm{h})$ gives the temperature of a drop on a fiber:

$$\Delta T^\star = \frac{1 + \tilde{\mathcal{Q}}_\mathrm{fiber} - \chi\alpha_1}{2\chi\alpha_2} - \frac{\sqrt{\left[1 + \tilde{\mathcal{Q}}_\mathrm{fiber} - \chi\alpha_1\right]^2 - 4\chi^2\alpha_2\,(1 - \mathcal{R}_\mathrm{H})}}{2\chi\alpha_2}, \tag{30}$$

From equation 30, asymptotic values for the temperature drop in the liquid can be obtained by comparing $\tilde{\mathcal{Q}}_\mathrm{fiber}$ with $1 - \kappa\alpha_1$.

For $\tilde{\mathcal{Q}}_\mathrm{fiber} \ll 1 - \chi\alpha_1$ we fine the case of an airborne sphere:

$$T_\infty - T_\mathrm{i} \approx \frac{1 - \chi\alpha_1 - \sqrt{(1 - \chi\alpha_1)^2 - 4\chi^2\alpha_2\,(1 - \mathcal{R}_\mathrm{H})}}{2\chi\alpha_2}. \tag{31}$$

For $\tilde{\mathcal{Q}}_\mathrm{fiber} \gg 1 - \chi\alpha_1$ we obtain :

$$T_\infty - T_\mathrm{i} \approx \frac{\kappa}{\tilde{\mathcal{Q}}_\mathrm{fiber}}(1 - \mathcal{R}_\mathrm{H}), \tag{32}$$

The two above equations are plotted, respectively in dash-dotted and dashed lines, in Figure 3(a) of the main text.

References

[1] B.J. Carroll. The accurate measurement of contact angle, phase contact areas, drop volume, and laplace excess pressure in drop-on-fiber systems. *Journal of Colloid and Interface Science*, 57(3):488 – 495, 1976.

[2] T.-H. Chou, S.-J. Hong, Y.-E. Liang, H.-K. Tsao, and Y.-J. Sheng. Equilibrium phase diagram of drop-on-fiber: Coexistent states and gravity effect. *Langmuir*, 27(7):3685–3692, 2011.

[3] G. McHale and M.I. Newton. Global geometry and the equilibrium shapes of liquid drops on fibers. *Colloids and Surfaces A: Physicochemical and Engineering Aspects*, 206(1-3):79–86, 2002.

[4] M. Corpart, F. Restagno, and F. Boulogne. Analytical prediction of the temperature and the lifetime of an evaporating spherical droplet. *Colloids and Surfaces A: Physicochemical and Engineering Aspects*, page 132059, 2023.

[5] D.R. Lide, editor. *CRC Handbook of Chemistry and Physics*. CRC Press/Taylor and Francis, 89th edition edition, 2008.

[6] E.N. Fuller, K. Ensley, and J.C. Giddings. Diffusion of halogenated hydrocarbons in helium. the effect of structure on collision cross sections. *The Journal of Physical Chemistry*, 73(11):3679–3685, 1969.

[7] E. N. Fuller, P. D. Schettler, and J. C. Giddings. New method for prediction of binary gas-phase diffusion coefficients. *Industrial & Engineering Chemistry*, 58(5):18–27, 1966.

[8] G. Jakli, P. Tzias, and W. A. Van Hook. Vapor pressure isotope effects in the benzene (b)–cyclohexane (c) system from 5 to 80° ci the pure liquids b-d 0, b-d 1, ortho-, meta-, and para-b-d 2, b-d 6, c-d 0, and c-d 12. ii. excess free energies and isotope effects on excess free energies in the solutions b-h 6/b-d 6, c-h 12/c-d 12, b-h 6/c-h 12, b-d 6/c-h 12, and b-h 6/c-d 12. *The Journal of Chemical Physics*, 68(7):3177–3190, 1978.

[9] M. W. Cook. Vapor Pressure Apparatus. *Review of Scientific Instruments*, 29(5):399–400, May 1958.

[10] S. Young. On the boiling points of the normal paraffins at different pressures. *Proceedings of the Royal Irish Academy. Section B: Biological, Geological, and Chemical Science*, 38:65–92, 1928.

[11] E. G. Linder. Vapor Pressures of Some Hydrocarbons. *The Journal of Physical Chemistry*, 35(2):531–535, February 1931.

[12] S. Young. CIV.—Vapour pressures, specific volumes, and critical constants of normal octane. *Journal of the Chemical Society, Transactions*, 77(0):1145–1151, January 1900.

[13] A. Dejoz, V. González-Alfaro, P. J. Miguel, and M. I. Vázquez. Isobaric Vapor–Liquid Equilibria for Binary Systems Composed of Octane, Decane, and Dodecane at 20 kPa. *Journal of Chemical & Engineering Data*, 41(1):93–96, January 1996.

[14] M.B. Ewing and J.C. Sanchez Ochoa. The vapour pressure of cyclohexane over the whole fluid range determined using comparative ebulliometry. *The Journal of Chemical Thermodynamics*, 32(9):1157–1167, September 2000.

[15] S. Weiguo, A. X. Qin, P. J. McElroy, and A. G. Williamson. (Vapour + liquid) equilibria of (n-hexane + n-hexadecane), (n-hexane + n-octane), and (n-octane + n-hexadecane). *The Journal of Chemical Thermodynamics*, 22(9):905–914, September 1990.

[16] G. F. Carruth and R. Kobayashi. Vapor pressure of normal paraffins ethane through n-decane from their triple points to about 10 mm mercury. *Journal of Chemical & Engineering Data*, 18(2):115–126, April 1973.

[17] T. N. Bell, E. L. Cussler, K. R. Harris, C. N. Pepela, and P. J. Dunlop. An apparatus for degassing liquids by vacuum sublimation. *The Journal of Physical Chemistry*, 72(13):4693–4695, December 1968.

[18] A. J. B. Cruickshank and A. J. B. Cutler. Vapor pressure of cyclohexane, 25 to 75.degree. *Journal of Chemical & Engineering Data*, 12(3):326–329, July 1967.

[19] A. Ksiazczak and J. J. Kosinski. Vapor pressure of solutions of polar aromatic compounds in cyclohexane at 298.15 and 323.15 K. *Journal of Chemical & Engineering Data*, 36(4):351–354, October 1991.

[20] E. R. Washburn and B. H. Handorf. The Vapor Pressure of Binary Solutions of Ethyl Alcohol and Cyclohexane at 25°. *Journal of the American Chemical Society*, 57(3):441–443, March 1935.

[21] F. J. Carmona, J. A. González, I. García de la Fuente, J. C. Cobos, V. R. Bhethanabotla, and S. W. Campbell. Thermodynamic Properties of n -Alkoxyethanols + Organic Solvent Mixtures. XI. Total Vapor Pressure Measurements for n -Hexane, Cyclohexane or n -Heptane + 2-Ethoxyethanol at 303.15 and 323.15 K. *Journal of Chemical & Engineering Data*, 45(4):699–703, July 2000.

[22] E. L. Andreas. The temperature of evaporating sea spray droplets. *J. Atmos. Sci.*, 52(7):852–862, 1995.

[23] N. A. Fuchs. *Evaporation and Droplet Growth in Gaseous Media*. Pergamon Press, London, 1959.

[24] B. Sobac, P. Talbot, B. Haut, A. Rednikov, and P. Colinet. A comprehensive analysis of the evaporation of a liquid spherical drop. *Journal of Colloid and Interface Science*, 438:306 – 317, 2015.

[25] K. V. Beard and H. R. Pruppacher. A wind tunnel investigation of the rate of evaporation of small water drops falling at terminal velocity in air. *J. Atmos. Sci.*, 28(8):1455 – 1464, 1971.

[26] R. R. Netz. Mechanisms of airborne infection via evaporating and sedimenting droplets produced by speaking. *J. Phys. Chem. B*, 124(33):7093–7101, August 2020.

[27] R. R. Netz and W. A. Eaton. Physics of virus transmission by speaking droplets. *Proc. Natl. Acad. Sci.*, 117(41):25209–25211, 2020.

[28] N. Frossling. Uber die verdunstung fallernder tropfen. *Gerlands Beitr. Geophys.*, 52:170–216, 1938.

[29] W. E. Ranz and W.R. Marshall. Evaporation from drops: Part II. *Chemical Engineering Progress*, 48(4):173–181, 1952.

[30] W. E. Ranz and W.R. Marshall. Evaporation from drops: Part I. *Chemical Engineering Progress*, 48(3):141–146, 1952.

[31] M. Corpart, J. Dervaux, C. Poulard, F. Restagno, and F. Boulogne. Evaporation of liquid coating a fiber. *Europhysics Letters*, 139(4):43001, August 2022.